

Planar silicon structure in application to the modulation of infrared radiation

TADEUSZ PIOTROWSKI^{1*}, DANIEL TOMASZEWSKI¹, MACIEJ WĘGRZECKI¹, VLADIMIR K. MALYUTENKO², ANDREW M. TYKHONOV²

¹Institute of Electron Technology, al. Lotników 32/46, 02-668 Warsaw, Poland

²Lashkaryov Institute of Semiconductor Physics, 45 Nauki Prospect, 03028 Kiev, Ukraine

*Corresponding author: piotrows@ite.waw.pl

We report on the performance of planar silicon diodes, operating at a temperature range above 300 K and emitting infrared radiation. The results present a theoretical analysis and experimental verification of an optimization aimed at a maximal difference between emissivity of this structure for cases with and without forward bias applied to $p-n$ junction. Several advantages of the structures were shown: wide emission spectrum (3–12 μm), short rise-fall time (300 μs), high operating temperature (≈ 400 K). Spatial distribution of photonic radiation emitted by a silicon structure obtained by a thermovision camera is compared with computer simulation distribution of carrier concentration. These planar sources can be used as easily controlled sources of infrared radiation in a wide spectral range, image simulators, *e.g.*, dynamic scene simulation devices with frame frequencies well above 200 Hz and for measurements of thermovision camera dynamic parameters.

Keywords: infrared radiation, emission, free carrier injection.

1. Introduction

The formation of dynamic infrared images has been reviewed in [1–3]. It has been shown recently [4–6] that indirect wide bandgap semiconductors could form a platform for photonic devices emitting infrared radiation (IR) in the wavelength range $\lambda = 3\text{--}12 \mu\text{m}$. In conventional light emitting diodes (LEDs), light comes as a result of interband radiative recombination of injected electrons and holes ($\lambda < hc/E_g$, where h is Plank's constant, c is light velocity, E_g is a band gap). In contrast to LEDs the described diode structure (emitting in the spectral band beyond the fundamental absorption edge, with $\lambda > hc/E_g$) exploits the increase in the emissivity ε of the diode base that is initially transparent at these wavelengths ($kd \ll 1$, where k is the absorption coefficient, d is the base thickness).

It is the emissivity modulation that makes the thermal emission (TE) of a base to change. More specifically, the TE power density emitted by an optically thin base,

$P_{\min} = \varepsilon W_B$, depends on the blackbody radiation density W_B (in the spectral range of interest) and emissivity $\varepsilon \approx (1 - R)(1 - \exp(kd))$, with R the reflection coefficient. This emissivity depends on the base thickness and on the absorption coefficient $k = \sigma_n n + \sigma_p p$, where σ_n , σ_p are the cross-sections of photon absorption by free concentrations of electrons (n) and holes (p), respectively.

The modulation of TE emission value in semiconductors induced by free carrier injection and exclusion processes and the practical application of this effect, are well documented in the literature [4–8].

In this paper, we report on the optimization and performance of a cost-effective Si structure that is prepared by the standard planar technology and can emit IR radiation.

2. Technology and experimental results

The sources (Fig. 1) under study were made of the $2\text{ k}\Omega\text{cm}$ FZ n -Si wafers with thickness of $300\text{--}500\text{ }\mu\text{m}$ and with nearly intrinsic (i) conductivity at $T > 400\text{ K}$. Both facets of the wafers were optically polished and chemically etched. Then, the standard thermal oxidation technique was applied for the reduction of surface recombination process. The 500-nm-thick SiO_2 dielectric layers on both facets of a wafer were grown in the atmosphere of dry oxygen. Planar junctions were fabricated on the front facet by standard optical lithography followed by conventional phosphorus ($n^+ - n$) and boron ($p^+ - n$) thermal diffusion processes. Contacts to the junctions were made by evaporating Al films. The $0.5 \times 0.5\text{ mm}$ $p^+ - n$ junction area was fabricated in the centre of the $6 \times 6\text{ mm}$ rectangular element and the 0.5-mm-wide $n^+ - n$ junction belt girdled the active area along its peripheral part (Fig. 1). Two sets of devices were fabricated and examined: both-side emitting structures and front-side emitting structures. The both-side emitting structures were covered with SiO_2 film from the both sides, while the front-side emitting structures were covered with the Al mirror deposited directly on the back facet of a structure covered with SiO_2 .

The structures were mounted on a copper heat-sink heater. By controlling the current in the heater circuit, the device heating (that was controlled by the thermocouple and

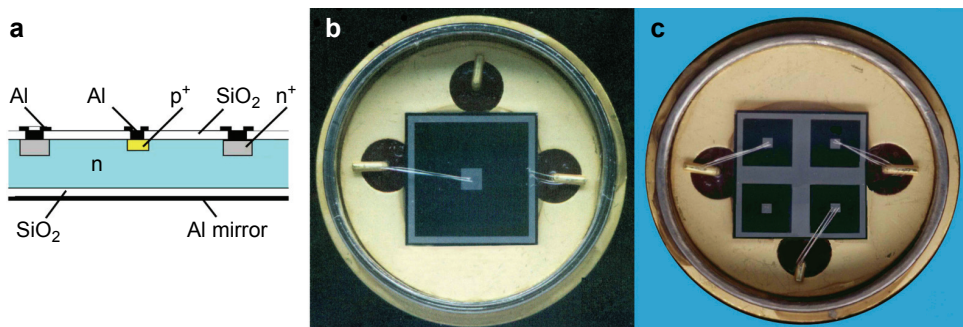


Fig. 1. Silicon planar source of infrared radiation: **a** – schematic cross-section of the emitting structure (not in scale); **b, c** – microphotographs of the single element and 2×2 array sitting on the metallic heater.

IR camera) was achieved up to 500 K. The TE patterns have been recorded by thermal imaging camera operating in the 3–5 μm band, while the time response was measured with a cooled HgMnTe photodetector sensitive in 8–12 μm band. Thermovision images were obtained using scanning thermovision cameras AGEMA and FLIR.

Experimental results are shown in Figs. 2–5. Figures 2–4 prove the facts of the injection of carriers from both sides (p^+ base and n^+ contact).

This image shows evidently that the double injection mode occurs, *i.e.*, carriers of both, n and p types, take part in the processes of emission and absorption of radiation. It causes a decrease in the density distribution of emitted radiation along the distance from the edge of p^+-n junction at the structure centre towards the half of the structure

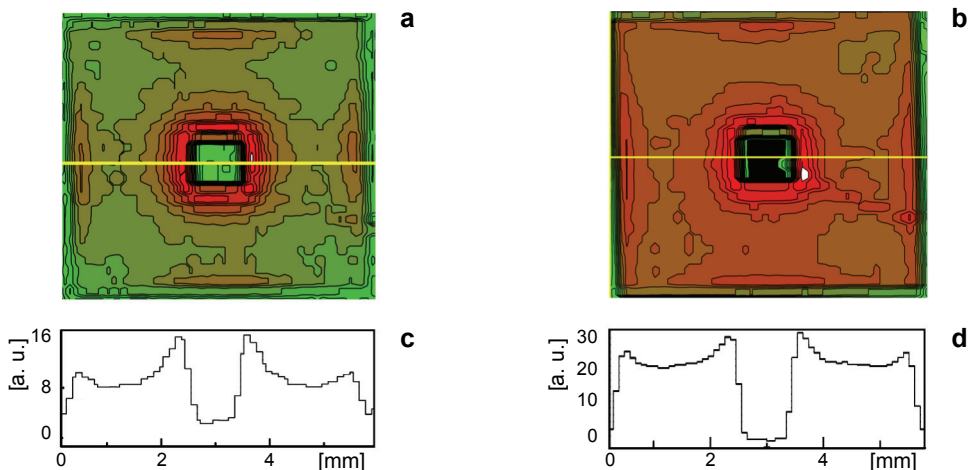


Fig. 2. Thermovision images of the manufactured source recorded at forward current 0.3 A (a), and 0.8 A (b) at temperature 400 K. Distribution of the radiant flux density (in arbitrary units) at current impulse, registered along a horizontal line from the left to the right at the structure centre (c, d).

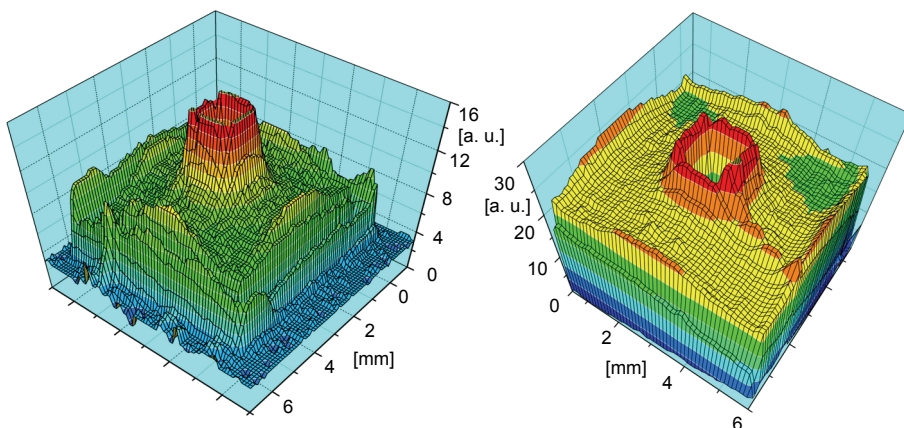


Fig. 3. The 3-D maps of free carrier injection process into the base of structure shown in Fig. 2 demonstrate a higher integral IR power emitted by the p^+-i-n^+ .

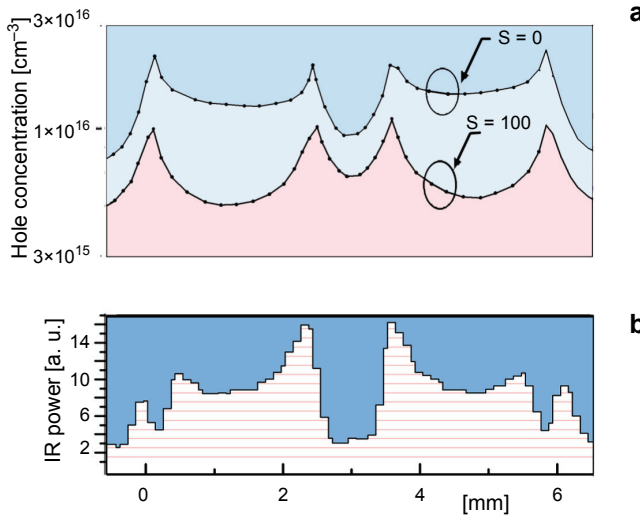


Fig. 4. Theoretical profiles of hole concentrations in the plane crossing the structure centre for $S = 0$ and 100 cm/sec on back surface (a) and experimental profile of emitted IR radiation (b). The reduction of radiation of near $n-n^+$ junction and $n-p^+$ junction results from massaging the radiation by the metallic contacts. The simulation has been performed using the Atlas program.

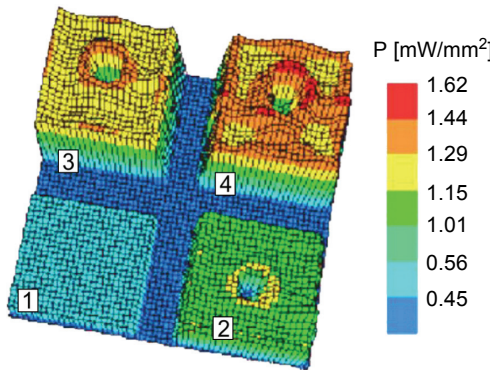


Fig. 5. The infrared radiation density of the four-element planar structure measured as a function of the current (1 – 0 A, 2 – 0.1 A, 3 – 0.3 A, 4 – 0.5 A, $T = 473 \text{ K}$).

radius, where the emission reaches its minimum. On the contrary, the emission density increases again at the boundaries of n^+-n junction (Figs. 2, 3). The density of emitted radiation is low at the square metallic region of contact to p^+ region at the structure centre, because the Al emissivity is comparatively low. A similar effect of decreased radiation density is observed at the region of Al contact to n^+ region along the outer edge of the structure. The radiation observed at the outer region beyond the metallic contact to n^+ region surrounding the structure results from the flow of carriers injected by the n^+-n junction, which occurs in both directions, towards p^+-n contact and outwards. This radiation is harmful in case of manufacturing of structure arrays,

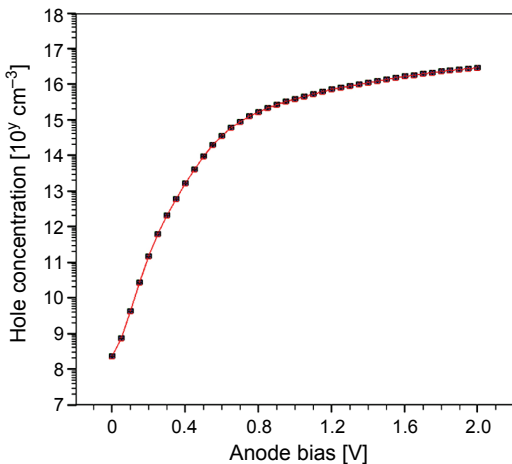


Fig. 6. The calculated I - V characteristic hole concentrations versus anode bias structure.

however it can be successfully suppressed by metallic layers deposited over the oxide. The integral power density of up to 3 mW and local power density up to 1 mW/mm^2 at $T = 473 \text{ K}$ were registered. These measurements were executed by a calibrated thermovision camera. The calculation I - V hole concentrations versus anode bias structure was showed in Fig. 6.

The results of performed simulation of current-carrier distribution are shown in Fig. 4. Changes in the carrier concentration in-depth of the structure, which were determined for the central region between anode and cathode, are indistinguishable [9]. Such distributions of carrier concentrations result from a high resistivity of the base and from a long lifetime of current carriers.

It can be observed in Figs. 2–4 that the radiation emitted by the structure is nonuniform. This effect occurs because the distance between the structure contacts exceeds the carrier diffusion length (which can be calculated from the carrier lifetime) by about 2–3 times. It is seen that the injected carriers recombine along their long path and their concentration significantly decreases with the increasing distance from the injecting contacts. These changes in the concentration influence the local emissivity, thus the local radiation power.

The mean emissivity of a source base was measured by the calibrated thermal imaging FLIR camera versus the bias current. It can be observed that the emissivity increases above 0.5 at high injection levels.

The density of infrared radiation (mW/mm^2) of four elements of a planar structure measured as a function of the current is shown in Fig. 5.

The theoretical emissivity was calculated assuming that the carrier lifetime in a diode base is equal to 1 ms, the excess-carrier concentration (determined by the bias current and the geometry of a structure) being the same as in the region close to the junction, the cross-section of photon absorption is equal to $1 \times 10^{-16} \text{ cm}^2$ and the absorption coefficient $k_1 = 0.2 \text{ cm}^{-1}$. Experimentally, at diode impulse current

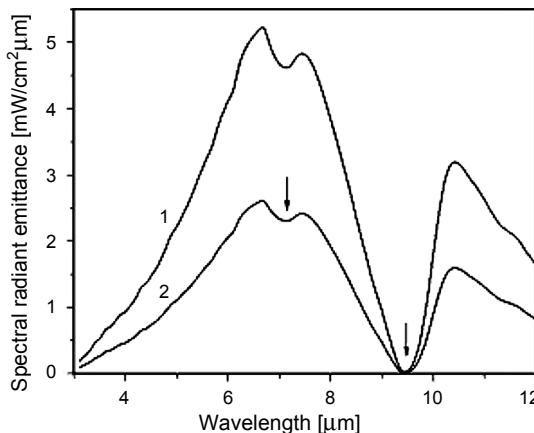


Fig. 7. Spectral radiant emittance distribution of the TE diode output at $T = 473$ K, $I = 0.8$ A (curve 1) and $I = 0.4$ A (curve 2). Two arrows show wavelength ranges where strong absorption bands exist.

equal to 0.8 A, the emissivity equal to 0.43 has been obtained, while the theoretical value calculated for this case is equal to 0.55. Concentration has been assumed as being constant in depth in the calculation.

Figure 7 shows the spectra (curves 1 and 2) of a single diode recorded at two values of a bias current. Two arrows on this spectrum show the fingerprints (absorption bands), which are due to the strong lattice absorption in Si ($7.1\text{ }\mu\text{m}$) and absorption in the thick SiO_2 films ($9.5\text{ }\mu\text{m}$).

Our tests have shown that Si planar structures based on the transparency modulation technique enhanced by the reflecting mirror on the back facet are easy to produce using well mastered silicon industrial technology.

The described silicon planar sources of modulated infrared radiation have the following advantages: widely distributed emission spectrum ($3\text{--}12\text{ }\mu\text{m}$), the record power conversion efficiency (up to 13%), the power output of 2–3 mW in both atmospheric transparency windows, the high operation temperature (that is limited by a quality of the $p\text{-}n$ junction), the very short rise-fall time ($300\text{ }\mu\text{s}$) [9] in comparison to other thermal emitters, and a low cost. These features make them an excellent choice for semiconductor modulators of infrared radiation as well as infrared radiation sources, radiation converters and image simulators, *e.g.*, IR dynamic scene simulation devices operating at frame frequencies well above 200 Hz. We expect that using antireflective ($R_1 < 10\%$) and highly reflective ($R_2 > 90\%$) facets can lead to a further increase in IR power output and increase in power conversion efficiency.

3. Summary

Our tests have shown that Si planar infrared diodes based on the transparency modulation technique enhanced by the reflecting mirror on the back facet are easy to produce using well mastered silicon industrial technology. The parameters of silicon

IR sources can be affected by the optimization of structure geometry including thicknesses, and by the optimization of passivation layers, which are used to avoid the presence of absorption bands as well as to modify spectral characteristics. An application of high-resistivity silicon, where the current-carrier lifetime is high, is needed to obtain a uniform carrier concentration in the whole volume of the structure base.

An application of the reflecting mirror on the back facet allows for increasing the emissivity by about 30% and manufacturing structures on thinner substrates. Thinner structures enable more uniform distribution of injected carriers and decrease the power supply. As a result, it was possible to obtain 60% emissivity change and fast reaction time. In case of the tested sources, the modulation frequency reached 2 kHz.

References

- [1] WILLIAMS O.M., REEVES G.K., ONG G.T., *Performance characteristics of thin film resistor arrays for infrared projector applications*, Proceedings of SPIE **1687**, 1992, pp. 71–81.
- [2] JOHNSON R.B., CHUNG R., GAITAN M., BERNING D., *Flat-panel thermal infrared scene generator*, Proceedings of SPIE **2269**, 1994, pp. 338–347.
- [3] COLE B.E., HIGASHI R.E., RIDLEY J.A., HOLMEN J., ARENDT J.W., MALONE C.L., STOCKBRIDGE R.G., GOLDSMITH G.C., JONES L.E., *512×512 WISP (wideband infrared scene projector) arrays*, Proceedings of SPIE **2741**, 1996, pp. 81–93.
- [4] MALYUTENKO V., MELNIK A., MALYUTENKO O., *High temperature ($T > 300$ K) light emitting diodes for 8–12 μm spectral range*, Infrared Physics and Technology **41**(6), 2000, pp. 373–378.
- [5] CHEN M.J., JEN J.L., LI J.Y., CHANG J.F., TSAI S.C., TSAI C.S., *Stimulated emission in a nano-structured silicon pn junction diode using current injection*, Applied Physics Letters **84**(12), 2004, pp. 2163–2165.
- [6] MALYUTENKO V.K., BOLGOV S.S., MALYUTENKO O.YU., *Above-room-temperature 3–12 μm Si emitting arrays*, Applied Physics Letters **88**(21), 2006, p. 211113.
- [7] LIPTUGA A., PIOTROWSKI T., SIKORSKI S., *Investigation of small-signal operation of the infrared germanium injection modulator*, Infrared Physics and Technology **38**(5), 1997, pp. 273–279.
- [8] MALYUTENKO V.K., *Thermal emission in semiconductors: Investigation and application*, Infrared Physics **32**, 1991, pp. 291–302.
- [9] PIOTROWSKI T., MALYUTENKO V.K., WĘGRZECKI M., CZERWINSKI A., POLAKOWSKI H., TYKHONOV A.M., *Optimization of parameters for silicon planar source of modulated infrared radiation*, Materials Science and Engineering B **176**(4), 2011, pp. 363–367.

Received September 25, 2010